

# Multivariable Fuzzy Decoupling Control of the Polymer Electromagnetism Dynamic Extrusion Process

Sheng-Ping Wen, Jing Jiang, Jin-Ping Qu, Gang Jin

National Engineering Research Center of Novel Equipment for Polymer Processing, College of Mechanical and Automotive Engineering, South China University of Technology, Guang Zhou 510640, China

Received 15 July 2008; accepted 21 September 2009

DOI 10.1002/app.31526

Published online 1 December 2009 in Wiley InterScience (www.interscience.wiley.com).

**ABSTRACT:** The plastic electromagnetism dynamic extruder has gained wide applications because of its novel structure and fine engineering performance. In the polymer processing, melt temperature and melt pressure control is crucial to the quality of the extruded product. A new multivariable fuzzy decoupling control algorithm of melt temperature and melt pressure for the novel extruder is introduced in the transfer function matrix system, which is obtained through the experimental data with system identification. To verify the application of the proposed control

algorithm, the multivariable closed-loop fuzzy decoupling system is implemented on programmable computer controller. Experimental results show melt temperature and melt pressure can be successful individually controlled by the heater power and the screw speed. The good system performance verifies the control strategy's validity. © 2009 Wiley Periodicals, Inc. *J Appl Polym Sci* 116: 568–576, 2010

**Key words:** extrusion; fuzzy decoupling control; melt temperature; melt pressure; multivariable

## INTRODUCTION

Polymer extrusion is a complex nonlinear multivariable coupling process. There are many factors affecting the stability of extrusion process and the quality of extruded products. The equipment is the crucial factor. There are already many kinds of extruder. Unlike the traditional extruder, a new kind of electromagnetism dynamic extruder was invented by Professor Qu Jinping.<sup>1</sup> He introduced the vibration force field into the whole process of polymer extrusion. The vibration force field brings new changes to the energy balance, quality balance and momentum balance of the whole extrusion process. Control of vibration frequency and vibration magnitude can effectively control the dynamic extrusion process. Researches on the dynamic extruder show the good performance of the machine.

Besides the extruder, control strategy is especially important. There were many literatures about extrusion process control,<sup>2–6</sup> i.e., temperature control, pressure control and viscosity control.<sup>7–13</sup> Control of the melt temperature and melt pressure were the most popular control approach to the extrusion pro-

cess. Melt pressure directly influences the output of the product. While melt temperature's fluctuation can affect melt viscosity and consequently influence melt pressure and flow rate. Therefore, melt temperature and melt pressure are the dominant variables in the dynamic extrusion process.

To get high-quality products, melt temperature and melt pressure for the traditional extruder have been proposed with different control methods. Dormeier firstly introduced the digital PID to melt temperature cascade control.<sup>14</sup> Rickey et al. used model prediction control (MPC) to establish the multiple-input multiple-output (MIMO) model of the temperature in different sections of the barrel.<sup>15</sup> Ching-Chin Tsai and Chi-Huang Lu investigated the multivariable temperature control of the barrel based on the generalized predictive algorithm.<sup>16</sup> Chi-Huang Lu also adopted the self-adaptive prediction control to the barrel temperature control.<sup>17</sup> Fabio et al.<sup>18</sup> designed three control subtasks: the inner-loop control of the local temperatures along the barrel; the outer-loop control of the temperature at the extruder output; the control of the pressure at the extruder output. Zengqiang et al.<sup>19</sup> applied a feedforward neural network to approximate the highly rigid plant with the learning algorithm of multivariable nonlinear least square method having fast convergence. In addition, a diversity of techniques has been employed<sup>20</sup>, including linear PI decoupling and MPC, as well as nonlinear geometric, MPC, and calorimetric control techniques, and the controllers

Correspondence to: S.-p. Wen (shpwen@scut.edu.cn) or J. Jiang (jiangjing0930@gmail.com).

Contract grant sponsor: National Natural Science Foundation of China; contract grant number: 10590351.

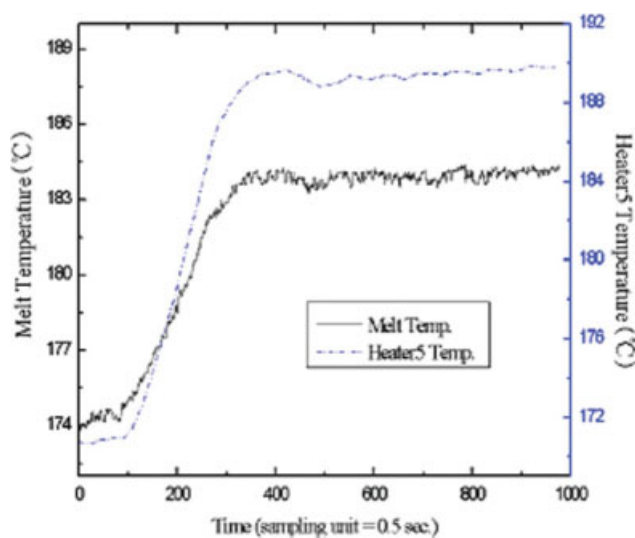


**Figure 1** Step response of melt temperature to barrel5 temperature. [Color figure can be viewed in the online issue, which is available at [www.interscience.wiley.com](http://www.interscience.wiley.com).]

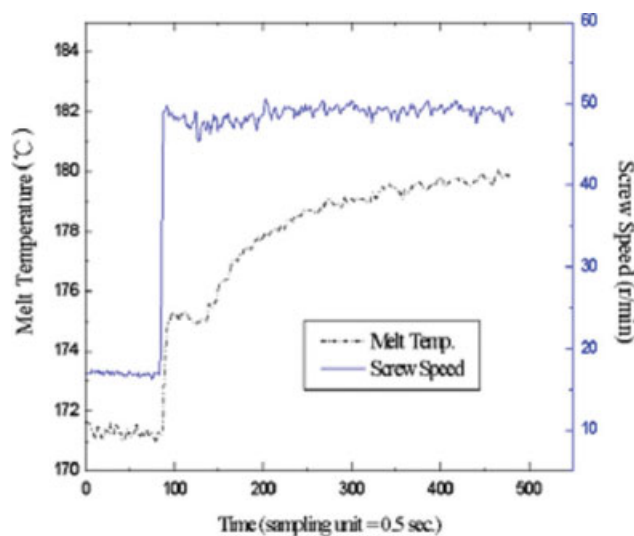


**Figure 2** Step response of melt temperature to screw speed. [Color figure can be viewed in the online issue, which is available at [www.interscience.wiley.com](http://www.interscience.wiley.com).]

have been implemented with open-loop, extended Kalman filter (EKF), and Luenberger nonlinear observers.

Achievements gained were mainly about the traditional extruder.<sup>21</sup> Melt temperature and melt pressure control of the electromagnetism dynamic extruder has seldom reported by now. In this article, a dynamic fuzzy self-adjusting decoupling controller is designed to remove the coupling effects between melt temperature and melt pressure in the electromagnetism dynamic extrusion process. This control strategy proposed is very easy to design and implement.

### SYSTEM IDENTIFICATION

The electromagnetism dynamic extruder has five heating zones. Temperatures of the first four heaters are set by manual. The temperature of the heater on the die is to be controlled by the new control strategy. There are five thermocouples positioned in the barrel-wall to measure the barrel wall temperature. One infrared temperature transducer is positioned nearest the exit of the die to measure melt temperature. Melt pressure is measured by a strain-gauge-type pressure transducer positioned in the die-wall. Melt pressure is controlled by screw speed. Step response of melt pressure and melt temperature to

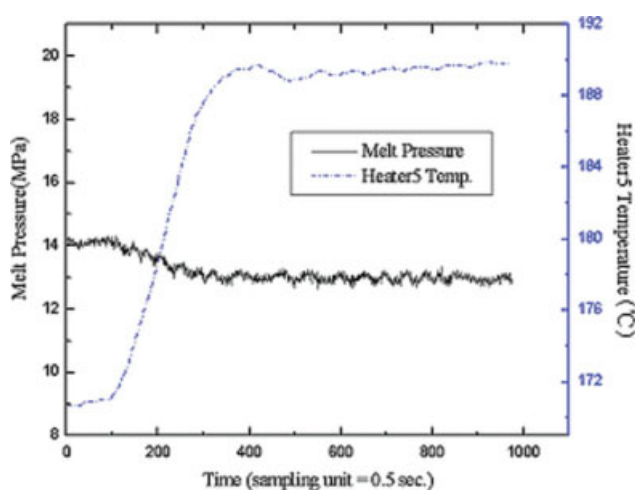


**Figure 3** Step response of melt pressure to barrel5 temperature. [Color figure can be viewed in the online issue, which is available at [www.interscience.wiley.com](http://www.interscience.wiley.com).]

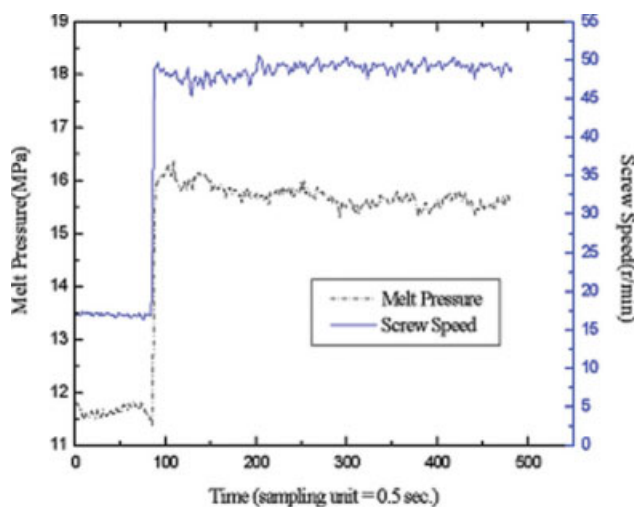


**Figure 4** Step response of melt pressure to screw speed. [Color figure can be viewed in the online issue, which is available at [www.interscience.wiley.com](http://www.interscience.wiley.com).]

TABLE I  
Step Response Data of Melt Temperature to Barrel 5 Temperature

| $t_i$    | 250    | 275    | 300    | 325   | 350    | 375     | 400     | 425     | 450     |
|----------|--------|--------|--------|-------|--------|---------|---------|---------|---------|
| $y_i(t)$ | 0.8712 | 0.9235 | 0.9607 | 0.975 | 0.9902 | 0.99518 | 0.99836 | 0.99913 | 0.99952 |

heater power on the die and screw speed were acquired through experiments. Figures 1–4 are experimental step responses of melt temperature and melt pressure.

Response of melt pressure and melt temperature to the heater power and screw speed is a self-balanced system. The response is over-damping. So the system is considered as a second order system and system parameters can be identified from experimental data.<sup>22</sup> The system model of melt temperature and melt pressure to the heater power and screw speed is expressed as following.

$$\begin{bmatrix} T_m(s) \\ P_m(s) \end{bmatrix} = \begin{bmatrix} G_{11} & G_{12} \\ G_{21} & G_{22} \end{bmatrix} \times \begin{bmatrix} W(s) \\ n(s) \end{bmatrix} \quad (1)$$

where  $T_m$ ,  $P_m$  are melt temperature and melt pressure.  $W$  represents the heater 5 power and  $n$  denotes the screw speed.  $G$  is the transfer function matrix. The transfer function of the second order self-balance system with a pure delay is expressed as following.

$$G(s) = \frac{Ke^{-\theta s}}{\tau^2 s + 2\xi\tau s + 1} \quad (2)$$

where  $K$  is the system gain,  $\theta$  is the delay time,  $\xi$  is the damping ratio,  $\tau$  is the time constant.  $K$  and  $\theta$  can be obtained directly from experimental data.  $\tau$  and  $\xi$  are computed by the following method.

The dimensionless transfer function without pure delay is described as:

$$G(s)^* = \frac{1}{\tau^2 s + 2\xi\tau s + 1} \quad (3)$$

which can be written in the following form:

$$G(s)^* = \frac{1}{\tau^2(s + \omega_1)(s + \omega_2)} \quad (4)$$

$$\begin{cases} \omega_1 = \frac{1}{\tau} \left[ \xi - \sqrt{\xi^2 - 1} \right] \\ \omega_2 = \frac{1}{\tau} \left[ \xi + \sqrt{\xi^2 - 1} \right] \end{cases} \quad (5)$$

Because of the step response of melt pressure and melt temperature is over-damping (i.e.  $\xi \geq 1$ ), eq. (5) is deduced as following

$$\begin{cases} \tau = \frac{1}{\sqrt{\omega_1\omega_2}} \\ \xi = \frac{\omega_1 + \omega_2}{2\sqrt{\omega_1\omega_2}} \end{cases} \quad (6)$$

Then  $\tau$  and  $\xi$  can be obtained by  $\omega_1$  and  $\omega_2$ . By using eq., (6) the step response of eq. (4) becomes:

$$1 - y^*(t) = \frac{\omega_2}{\omega_2 - \omega_1} e^{-\omega_1 t} - \frac{\omega_1}{\omega_2 - \omega_1} e^{-\omega_2 t} \quad (7)$$

Supposing  $\omega_2 = \alpha\omega_1$ , ( $\alpha \geq 1$ ) eq. (7) can be represented as

$$\log(1 - y^*(t)) = \log \frac{\alpha}{\alpha - 1} - 0.4343\omega_1 t \quad (8)$$

Using  $y(t) = at + b$ , eq. (8) becomes

$$y(t) = \log(1 - y^*(t)), \quad a = -0.4343\omega_1, \quad b = \log \frac{\alpha}{\alpha - 1} \quad (9)$$

Using the least square principle, the following equation groups are obtained:

$$\begin{cases} a = \frac{n \sum_{i=1}^n t_i y_i(t) - \sum_{i=1}^n t_i \sum_{i=1}^n y_i(t)}{n \sum_{i=1}^n t_i^2 - \sum_{i=1}^n t_i \sum_{i=1}^n t_i} \\ b = \frac{\sum_{i=1}^n y_i(t) - a \sum_{i=1}^n t_i}{n} \end{cases} \quad (10)$$

Then,  $\tau$  and  $\xi$  in the eq. (3) can be obtained from eqs. (8–10).

The dimensionless experimental data of step response of melt pressure and melt temperature can be acquired in the Figures 1–4, showing as Tables I–IV, respectively.

The transfer function of  $G^*$  can be identified from the experimental data in Tables I–IV.

$$G_{11}^*(s) = \frac{1}{(58.8 s + 1)^2} \quad (11)$$

TABLE II  
Step Response Data of Melt Temperature to Screw Speed

| $t_i$    | 82      | 107     | 132     | 157     | 182     | 207     | 232     | 257     |
|----------|---------|---------|---------|---------|---------|---------|---------|---------|
| $y_i(t)$ | 0.84323 | 0.88889 | 0.92568 | 0.94988 | 0.97775 | 0.98976 | 0.99851 | 0.99963 |

**TABLE III**  
Step Response Data of Melt Pressure to Barrel 5 Temperature

|          |        |        |       |       |        |        |        |        |        |
|----------|--------|--------|-------|-------|--------|--------|--------|--------|--------|
| $t_i$    | 225    | 250    | 275   | 300   | 325    | 350    | 375    | 400    | 425    |
| $y_i(t)$ | 0.8506 | 0.8875 | 0.924 | 0.954 | 0.9765 | 0.9893 | 0.9956 | 0.9983 | 0.9995 |

$$G_{12}^{*'}(s) = \frac{0.004366}{(s + 0.01964)(s + 0.2223)} \quad (12)$$

$$G_{21}^{*'}(s) = \frac{-1}{(56s + 1)^2} \quad (13)$$

$$G_{22}^{*'}(s) = \frac{13.76}{(s + 3.71)^2} \quad (14)$$

According to experimental data,  $k_{11} = 1.8$  and  $\theta_{11} = 15s$ .

$$k_{12} = \frac{\Delta T_m}{\Delta n} = \frac{179.8 - 171.3}{47.53 - 18.05} = \frac{8.5}{29.48} = 0.29 \quad (15)$$

$$k_{21} = \frac{\Delta P_m}{\Delta T_m} \cdot k_{11} = \frac{12.92 - 14.13}{184 - 174} \times 1.8 = -0.22, \quad \theta_{21} \approx \theta_{11} + 10s = 25s \quad (16)$$

and

$$k_{22} = \frac{P_m(\infty)}{n} = \frac{13.655}{29} = 0.47 \quad (17)$$

Finally, the transfer function matrix of the system model of melt temperature and melt pressure to the heater power and screw speed is obtained as:

$$\begin{bmatrix} T_m(s) \\ P_m(s) \end{bmatrix} = \begin{bmatrix} \frac{1.8e^{-15s}}{(58.8s+1)^2} & \frac{0.29}{(50.92s+1)(4.5s+1)} \\ \frac{-0.22e^{-25s}}{(56s+1)^2} & \frac{0.47}{(0.27s+1)^2} \end{bmatrix} \times \begin{bmatrix} W(s) \\ n(s) \end{bmatrix} \quad (18)$$

**FUZZY DECOUPLING CONTROL ALGORITHM**

According to the coupling relationship of melt temperature and melt pressure, we bring about a fuzzy decoupling controller for melt temperature and melt pressure control shown in Figure 5.

Where  $T_m$  and  $P_m$  are the actual outputs of melt temperature and melt pressure.  $T_{mset}$  and  $P_{mset}$  are the set points of melt temperature and melt pressure. The whole system consists of fuzzy logic controller (FLC), decoupling compensator unit and

fuzzy adjusting components unit. Decoupling coefficients vary according to the fuzzy adjusting components, so that the coupling of the two loops can be eliminated.

**MIMO FLC design**

Design of FLC1 is the same as that of FLC2, so we only introduce the design of FLC1. Two dimension fuzzy controllers is adopted. Inputs of the fuzzy controller are error (E) and ratio of error change (EC). Output (U) is the control signal sent to the plant. Fuzzy sets of E, EC, and U are defined as {NB, NM, NS, ZO, PS, PM, PB} (NB-negative big, NM, negative medium; NS, negative small; ZO, zero; PS, positive small; PM, positive medium; PB, positive big, and universe is chosen as {-6, -5, -4, -3, -2, -1, 0, 1, 2, 3, 4, 5, 6}. The membership function is the triangular function.

In the dynamic extrusion process, we have gained such experimental rules as "if temperature is low, rising of temperature is slow, then increase the heater power," and "if temperature is high, rising of temperature is quick, then the heater should be stopped," etc. Based on these manual experiences, the fuzzy linguistic rules are expressed as following

1. If E = NB or NM and EC = NB or NM then U = PB
2. If E = NB or NM and EC = NS or ZO then U = PB
3. If E = NB or NM and EC = PS then U = PM
4. If E = NB or NM and EC = PM or PB then U = ZO
5. If E = NS and EC = NB or NM then U = PM
6. If E = NS and EC = NS or ZO then U = PM

According to these rules, the fuzzy control Table is given in Table V.

Considering the multivariable system in this study has two inputs and two outputs, the following fuzzy model is obtained<sup>23</sup>:

**TABLE IV**  
Step Response Data of Melt Pressure to Screw Speed

|          |         |         |         |         |         |         |         |         |
|----------|---------|---------|---------|---------|---------|---------|---------|---------|
| $t_i$    | 1.2     | 1.35    | 1.5     | 1.65    | 1.8     | 1.95    | 2.1     | 2.25    |
| $y_i(t)$ | 0.88025 | 0.93407 | 0.96154 | 0.98231 | 0.99230 | 0.99615 | 0.99808 | 0.99923 |

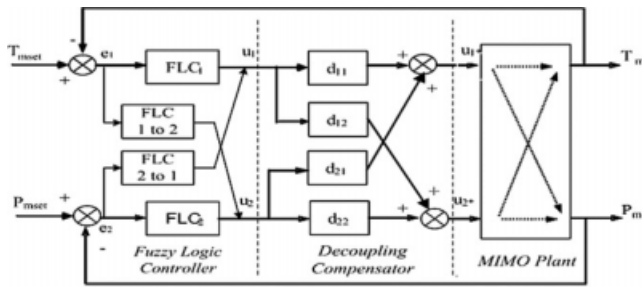


**Figure 5** the structure diagram of the melt temperature and melt pressure fuzzy decoupling system.

$$\begin{cases} u_1 = e_1^\circ R_{11} \wedge e_2^\circ R_{21} \\ u_2 = e_1^\circ R_{12} \wedge e_2^\circ R_{22} \end{cases} \quad (19)$$

$$\begin{bmatrix} u_1 \\ u_2 \end{bmatrix} = [e_1 \quad e_2] \times \begin{bmatrix} R_{11} & R_{21} \\ R_{21} & R_{22} \end{bmatrix} \quad (20)$$

where  $\circ$  is the max-min composition of fuzzy relation and  $\wedge$  is the min-operator,  $e_i$  is system input,  $u_i$  is the system output,  $R_{ij}$  are two-dimensional (flat) fuzzy relations and

$$R = \bigvee_{i=1}^2 \{e_i \wedge u_i\}$$

**Decoupling under steady state**

Under steady state, according to the mathematical model given in eq. (18), the steady-state gain matrix can be written as:

$$g = \begin{bmatrix} g_{11} & g_{12} \\ g_{21} & g_{22} \end{bmatrix} = \begin{bmatrix} 1.8 & 0.29 \\ -0.22 & 0.47 \end{bmatrix} \quad (21)$$

According to the principle of decoupling compensator,<sup>24</sup> steady-state decoupling coefficients matrix  $d$  is expressed as

$$d = \begin{bmatrix} d_{11} & d_{12} \\ d_{21} & d_{22} \end{bmatrix} = \begin{bmatrix} 1 & -\frac{g_{12}}{g_{11}} \\ -\frac{g_{21}}{g_{22}} & 1 \end{bmatrix} \quad (22)$$

From eqs. (21) and (22), the decoupling coefficients matrix under steady state is given

$$d = \begin{bmatrix} 1 & -0.161 \\ 0.468 & 1 \end{bmatrix} \quad (23)$$

**Fuzzy self-adjusting decoupling in dynamic process**

Decoupling coefficients  $d_{ij}$  ( $i, j = 1, 2$ ) mentioned above can only remove the coupling of melt temperature and melt pressure under steady state. To eliminate the coupling in dynamic process, decoupling coefficients should be regulated. The modification unit is depicted in Figure 6.

The modification unit in dynamic process can be written as below:

$$\begin{bmatrix} \Delta y_1 \\ \Delta y_2 \end{bmatrix} = \begin{bmatrix} \alpha_{11} & \alpha_{12} \\ \alpha_{21} & \alpha_{22} \end{bmatrix} \begin{bmatrix} u_1 \\ u_2 \end{bmatrix} \quad (24)$$

where  $u_i$  ( $i = 1, 2$ ) is the outputs of fuzzy controllers,  $\Delta y_i$  ( $i = 1, 2$ ) denotes the increment under dynamic state.  $\alpha_{ij}$  ( $i = 1, 2; j = 1, 2$ ) is the adjusting coefficients.

According to the description (24), the output increment  $\Delta y_i$  at time step  $n - 1$  and  $n$  are obtained

$$\Delta y_1(n - 1) = \alpha_{11}u_1(n - 2) + \alpha_{12}u_2(n - 2) \quad (25)$$

$$\Delta y_1(n) = \alpha_{11}u_1(n - 1) + \alpha_{12}u_2(n - 1) \quad (26)$$

**TABLE V**  
Fuzzy Control Rules of a Coupling FLC

| U | EC | -6 | -5 | -4 | -3 | -2 | -1 | 0  | 1  | 2  | 3  | 4  | 5  | 6  |
|---|----|----|----|----|----|----|----|----|----|----|----|----|----|----|
| E | -6 | 6  | 6  | 6  | 6  | 6  | 6  | 6  | 5  | 4  | 2  | 0  | 0  | 0  |
|   | -5 | 6  | 6  | 6  | 6  | 6  | 6  | 6  | 5  | 4  | 2  | 0  | 0  | 0  |
|   | -4 | 6  | 6  | 6  | 6  | 6  | 6  | 6  | 5  | 4  | 2  | 0  | 0  | 0  |
|   | -3 | 5  | 5  | 5  | 5  | 5  | 5  | 5  | 3  | 2  | 1  | -1 | -1 | -1 |
|   | -2 | 4  | 4  | 4  | 4  | 4  | 4  | 4  | 2  | 0  | -1 | -2 | -2 | -2 |
|   | -1 | 4  | 4  | 4  | 3  | 3  | 2  | 2  | 1  | -1 | -2 | -3 | -3 | -3 |
|   | 0  | 4  | 4  | 4  | 3  | 2  | 1  | 0  | -1 | -2 | -3 | -4 | -4 | -4 |
|   | 1  | 3  | 3  | 3  | 2  | 1  | -1 | -2 | -2 | -3 | -3 | -4 | -4 | -4 |
|   | 2  | 2  | 2  | 2  | 1  | 0  | -2 | -4 | -4 | -4 | -4 | -4 | -4 | -4 |
|   | 3  | 1  | 1  | 1  | -1 | -2 | -3 | -5 | -5 | -5 | -5 | -5 | -5 | -5 |
|   | 4  | 0  | 0  | 0  | -2 | -4 | -5 | -6 | -6 | -6 | -6 | -6 | -6 | -6 |
|   | 5  | 0  | 0  | 0  | -2 | -4 | -5 | -6 | -6 | -6 | -6 | -6 | -6 | -6 |
|   | 6  | 0  | 0  | 0  | -2 | -4 | -5 | -6 | -6 | -6 | -6 | -6 | -6 | -6 |

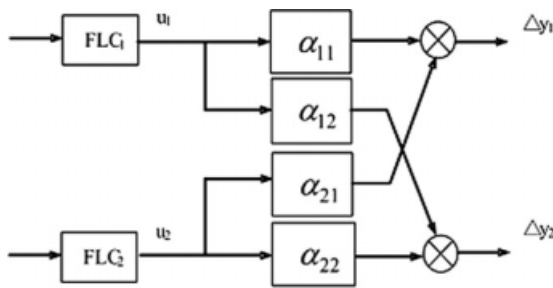


Figure 6 Adjusting compensator in dynamic process.

Substituting eq. (26) into eq. (25), we obtain

$$\alpha_{12} = \frac{\Delta y_1(n-1)u_1(n-1) - \Delta y_1(n)u_1(n-2)}{u_2(n-2)u_1(n-1) - u_2(n-1)u_1(n-2)} \quad (27)$$

Similarly,  $\alpha_{21}$  is given by

$$\alpha_{21} = \frac{\Delta y_2(n-1)u_2(n-1) - \Delta y_2(n)u_2(n-2)}{u_1(n-2)u_2(n-1) - u_1(n-1)u_2(n-2)} \quad (28)$$

To eliminate the coupling between the two closed-loops in dynamic process, it must let  $a_{ij} = 0$  ( $i = 1, 2; j = 1, 2; i \neq j$ ). If  $\alpha_{ij} \neq 0$  ( $i = 1, 2; j = 1, 2; i \neq j$ ), it means that decoupling coefficients is unreasonable. Decoupling coefficients are adjusted according to modifying coefficient by fuzzy logic. Fuzzy sets of decoupling coefficients and modifying coefficients are defined as {NB, NS, ZO, PS, PB}. The fuzzy control rule table of adjusting decoupling coefficients is shown in Table VI.

### IMPLEMENTATION OF THE CONTROL SYSTEM AND EXPERIMENTAL RESULTS

#### Implementation of the control system

Hardware design of the control system includes the choice of the master controller, design of the interface circuit, design of the drive and amplifier circuit, and design of hand machine interface (HMI). According to the control requirements and the characteristics of the plant, B and R PCC2003 is chosen as the master controller. Programmable computer controller (PCC) has the standard functions of the

TABLE VI  
Fuzzy rules for adjusting coefficients opposite decouple coefficients

|   |    |    |    |    |    |
|---|----|----|----|----|----|
| Adjusting coefficients ( $\alpha_{12}, \alpha_{21}$ ) | NB | NS | ZO | PS | PB |
| Decoupling coefficients ( $d_{12}, d_{21}$ )          | PB | PS | ZO | NS | NB |

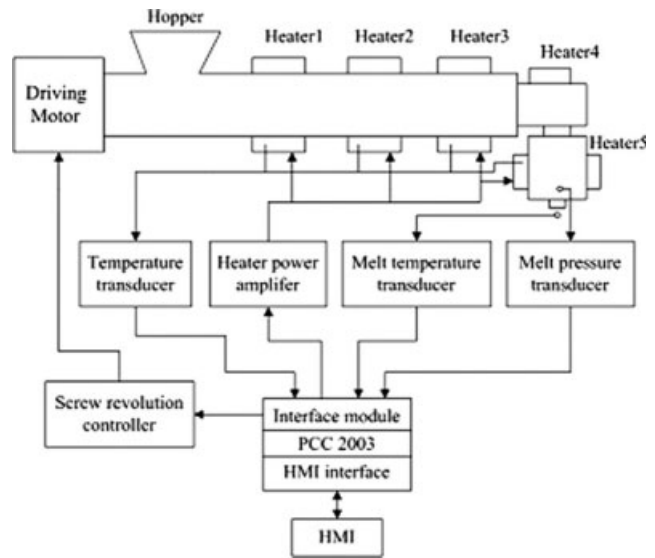


Figure 7 Configuration of the control system.

Programmable logic controller (PLC) and has the time division multiplexing operating system of the industry computer. PCC can conveniently process the analogous and digital signals and is easy to configuration because of its modular structure. Program based on PCC can be developed with the advanced language and mixture of different languages. The configuration is shown in Figure 7.

The control purpose is to bring the set points during startup as soon as possible while avoiding coupling influence and large overshoots, and to test the robustness of the proposed method. The following experiments were performed to observe whether these goals were achieved. In all experiments, the real-time multivariable fuzzy self-adjusting

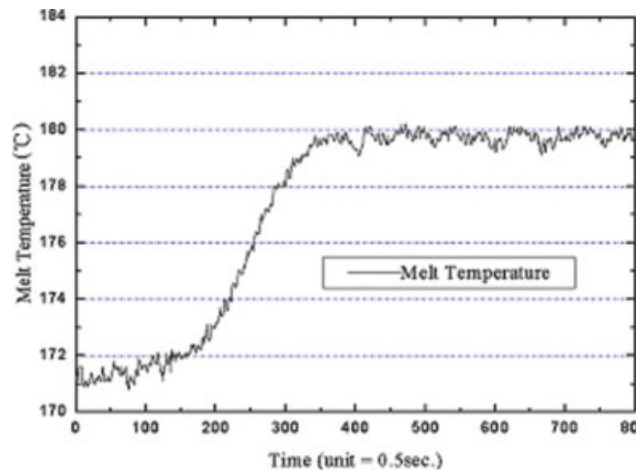
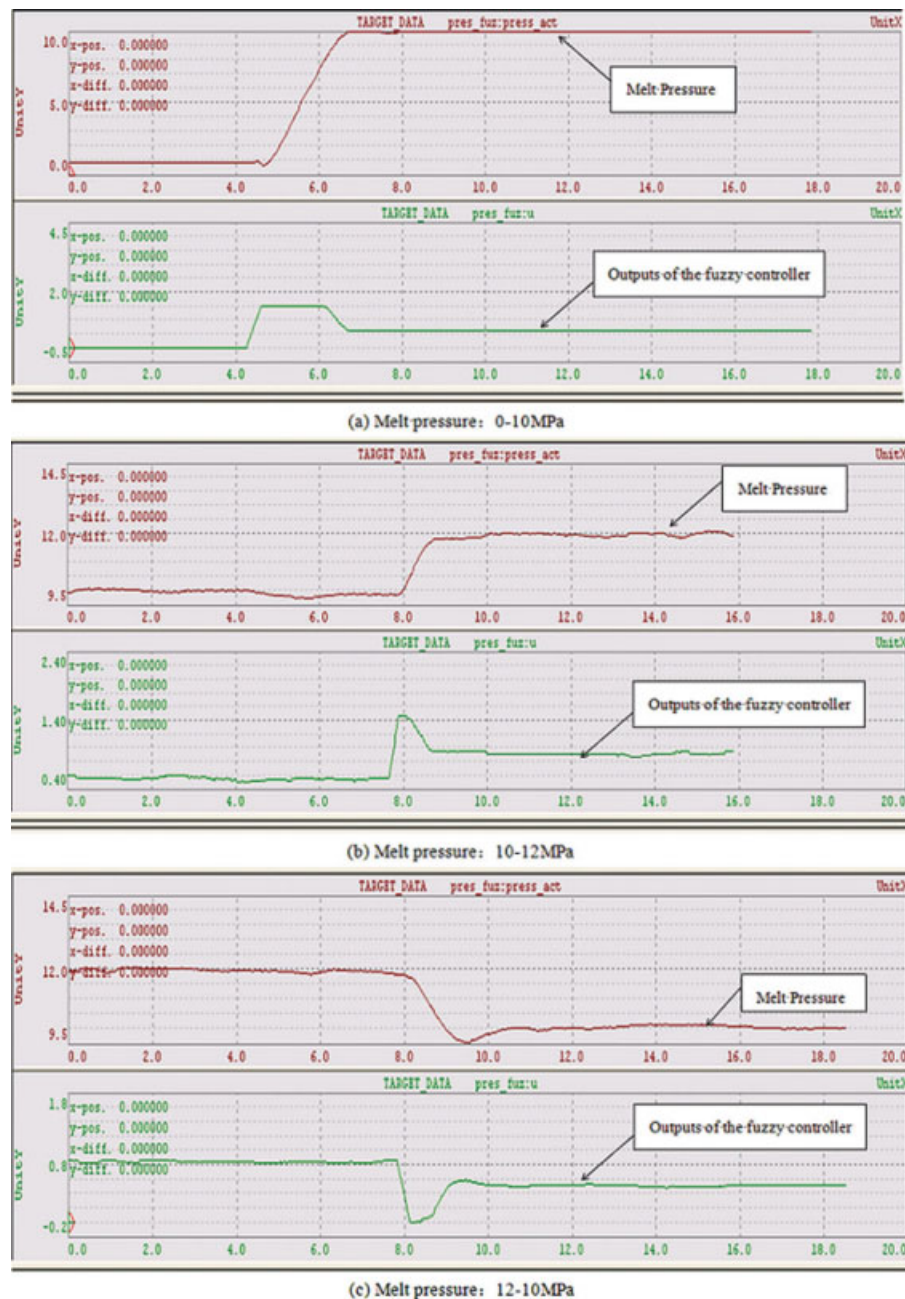


Figure 8 Fuzzy control response of melt temperature. [Color figure can be viewed in the online issue, which is available at www.interscience.wiley.com.]



**Figure 9** Fuzzy control response of melt pressure. [Color figure can be viewed in the online issue, which is available at [www.interscience.wiley.com](http://www.interscience.wiley.com).]

decoupling control algorithm present in “Fuzzy decoupling control algorithm” was implemented by using C language programming on Automation Studio (AS) software. The sampling period of melt temperature control is set to 0.5 s, while melt pressure’s is set to 20 ms.

### Experimental results

LLDPE is chosen as experimental material. The temperatures of heater 1–4 are set to be 165°C, 180°C, 180°C, and 175°C individually.

Steady-state responses of single-variable

Melt pressure is set to be 10 MPa and melt temperature is set to be 180°C. In Figure 8, melt temperature is controlled directly by the heater5 power under steady-state. It shows that temperature can quickly come to the set point when melt temperature is changed from 170 to 180°C. The steady-state errors remain less than 1°C and the rise-time is approximate 200 s. In Figure 9, Melt pressure is regulated by the screw speed. Figure 9(a–c) show the response curve of melt pressure. The steady-state errors are

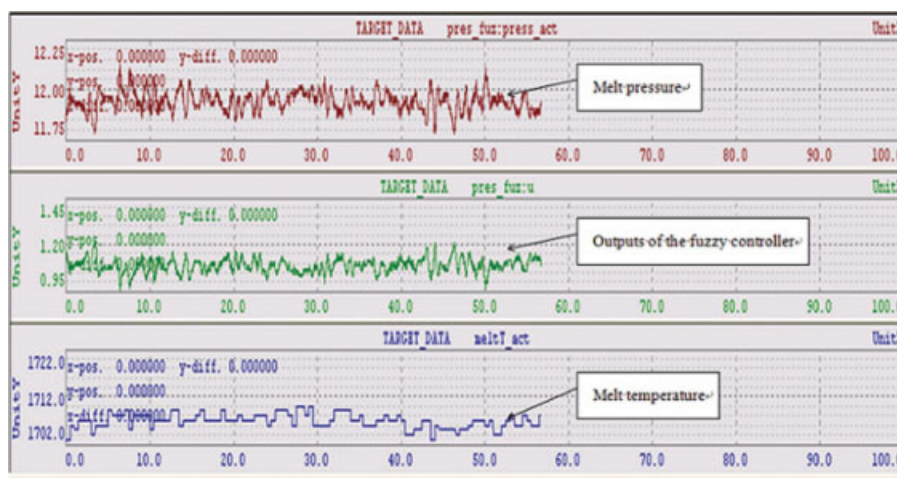


**Figure 10** Fuzzy decoupling control response of melt temperature and melt pressure. [Color figure can be viewed in the online issue, which is available at [www.interscience.wiley.com](http://www.interscience.wiley.com).]

less than 0.16 Mpa and the rise-time is approximate 2 s.

Steady-state decoupling

Melt pressure is set to be 12 Mpa and melt temperature is set to be 170°C. The 1702.0 in Figure 10 means 170.2°C. Figure 10 shows that the steady-state coupling between melt temperature and melt pressure is eliminate mostly. The steady-state errors of melt pressure is 0.15 Mpa and steady-state errors of melt temperature is about 0.9°C.

Dynamic decoupling

Melt pressure is set to be 10 Mpa and melt temperature is set to be 170°C. When the operation

becomes stable, melt pressure is changed to 12 Mpa. Figure 11 shows that actual pressure can quickly come to the set point while temperature remains to be 170°C. Figure 12 shows that when melt temperature set point is changed to be 180°C, the response of melt temperature is quick. Melt temperature comes to the set point while melt pressure is almost remain unchanged. Figure 3 shows that the effect of the open loop control and melt pressure decreases rapidly with the rise of melt temperature. After adopting the fuzzy logic decoupling control, Figure 12 verifies the validity of the new control method and melt pressure remains constant despite the variability of melt temperature. The case is the same to melt temperature versus variability of melt pressure and details are omitted here.

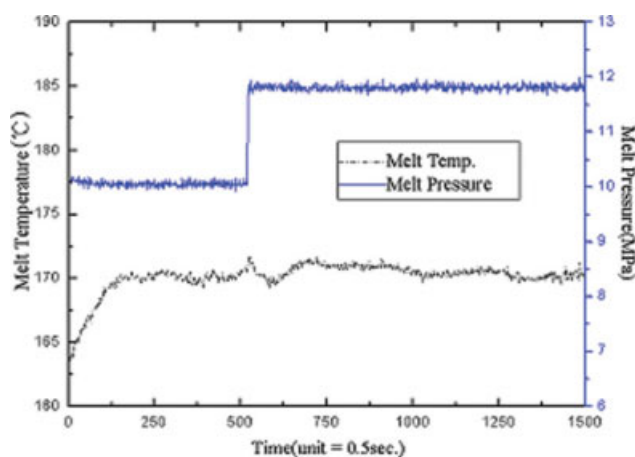


**Figure 11** Fuzzy decoupling response of melt pressure and melt temperature under melt pressure changing from 10 to 12 Mpa. [Color figure can be viewed in the online issue, which is available at [www.interscience.wiley.com](http://www.interscience.wiley.com).]

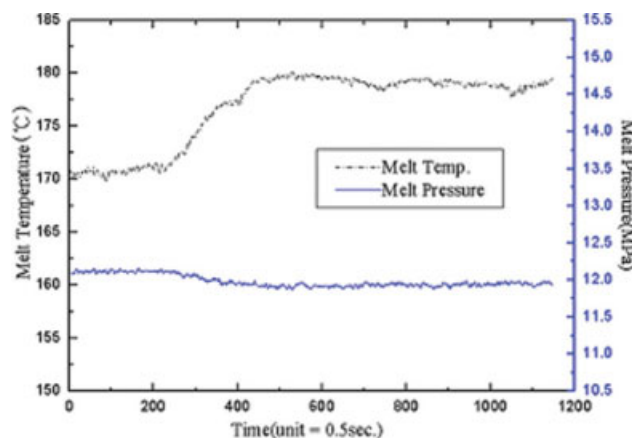


**Figure 12** Fuzzy decoupling response of melt temperature and melt pressure under melt temperature rising from 170 to 180°C. [Color figure can be viewed in the online issue, which is available at [www.interscience.wiley.com](http://www.interscience.wiley.com).]



## CONCLUSIONS

This article investigated the decoupling control of melt pressure and melt temperature for the electromagnetism dynamic extruder. A new control algorithm based on fuzzy logic is introduced, which consists of fuzzy controller, decoupling compensator unit and fuzzy self-adjusting components unit. Experimental results show that the multivariable decoupling controller meets the following performance specifications: (1) all steady-state errors remain with a low range for arbitrary constant command references and disturbances; (2) all overshoots are small; (3) the controller is robust for a range of parameter variations; (4) the coupling between melt temperature and melt pressure can be eliminated mostly. The validation of the fuzzy decoupling control strategy is verified. This control strategy can be also applied in the traditional extrusion process.

## NOMENCLATURE

|          |  |
|----------|--|
| $T_m$    | melt temperature                                   |
| $P_m$    | melt pressure                                      |
| $W$      | heater5 power                                      |
| $n$      | screw speed  |
| $G$      | transfer function matrix                           |
| $G^*$    | dimensionless transfer function without pure delay |
| $K$      | system gain  |
| $\theta$ | delay time   |
| $\xi$    | damping ratio                                      |
| $\tau$   | natural period (time constant)                     |

## References

1. Qu, J. *China Plastics* 1997, 11, 69.
2. Fodil-Pacha, F.; Arhaliass, A.; Aït-Ahmed, N.; Boillereaux, L.; Legrand, J. *Food Control* 2007, 18, 1143.
3. Chen, Z.-L.; Chao, P.-Y.; Chiu, S.-H. *Polym Test* 2003, 22, 601.
4. Tadmor, Z.; Klen, I. *Engineering Principles of Plasticating Extrusion*; Van Nostrand Reinhold Company: New York, 1970.
5. Tham, Y. W.; Fu, M. W.; Hng, H. H.; Yong, M. S.; Lim, K. B. *J Mater Process Technol* 2007, 192, 121.
6. Ke, Y.; Furong, G.; Frank, A. *Control Eng Prac* 2008, 16, 1259.
7. Hassan, G. A. Ph.D. Thesis, University of Bradford, 1979.
8. Han-Xiong, H.; Yu-Zhou, L.; Yan-Hong, D. *Polym Test* 2006, 25, 839.
9. Ajiboye, J. S.; Adeyemi, M. B. *Int J Mech Sci* 2008, 3, 522.
10. Gino, F.; Roberto, M. *J Food Eng* 2007, 83, 84.
11. Chiu, S. H.; Pong, S. H. *J Appl Polym Sci* 2001, 79, 1249.
12. Jing, J.; Shengping, W. *CCCM* 2008, 2, 172.
13. Béreaux, Y.; Charmeau, J.-Y.; Moguedet, M. *J Mater Process Technol* 2008, 209, 611.
14. Dormeier, S. *Extruder control*, IFAC PRP 4 Automation, Ghent, Belgium 1980, 551.
15. Rickey, D.; Adam, C. B.; Yash, P. G. *Polym Eng Sci* 1997, 37, 1150.
16. Ching-Chih, T.; Chi-Huang, L. *IEEE Trans Ind Appl* 1998, 34, 310.
17. Chi-Huang, L.; Ching-Chih, T. *IEEE Trans Ind Electron* 2001, 48, 968.
18. Fabio, P.; Sergio, M. S.; Angiolino, P. *Control Eng Prac* 2006, 14, 1111.
19. Zengqiang, C.; Xiang, L.; Zhongxin, L.; Zhuzhi, Y. *Chaos Solitons Fractals*, 2008, 35, 808.
20. Jesus, A.; Pablo, G. *J Process Control* 2007, 17, 463.
21. Seung, J. L.; Chang-Gi, H.; Tack-Su, H.; Jun-Young, K.; Young, A. K. *Food Control* 2002, 13, 301.
22. Zhi-an, S.; Wen-xin, W. *J Shandong University of Science Technology (Natural Science)*, 2003, 22, 61.
23. Gupta, M.; Jerzy, B. K.; Trojan, G. M. *IEEE Trans Sys Man Cybernetics* 1986, 5, 638.
24. Hongbo, L.; Shaoyuan, L.; Tianyou, C. *Electr Power Energy Syst* 2003, 25, 809.